Electronic and Optical Properties of Small Metal Fluoride Clusters

Giancarlo Cappellini,* Andrea Bosin, Giovanni Serra, Jürgen Furthmüller, Friedhelm Bechstedt, and Silvana Botti

Cite This: https://dx.doi.org/10.1021/acsomega.0c01317

Read Online

ACCESS | Metrics & More | Article Recommendations | SI Supporting Information

ABSTRACT: We report a systematic investigation on the electronic and optical properties of the smallest stable clusters of alkaline-earth metal fluorides, namely, MgF_2, CaF_2, SrF_2, and BaF_2. For these clusters, we perform density functional theory (DFT) and time-dependent DFT (TDDFT) calculations with a localized Gaussian basis set. For each molecule ($(MF_2)_n$, $n = 1-3$, M = Mg, Ca, Sr, Ba), we determine a series of molecular properties, namely, ground-state energies, fragmentation energies, electron affinities, ionization energies, fundamental energy gaps, optical absorption spectra, and exciton binding energies. We compare electronic and optical properties between clusters of different sizes with the same metal atom and between clusters of the same size with different metal atoms. From this analysis, it turns out that MgF_2 clusters have distinguished ground-state and excited-state properties with respect to the other fluoride molecules. Sizeable reductions of the optical onset energies and a consistent increase of excitonic effects are observed for all clusters under study with respect to the corresponding bulk systems. Possible consequences of the present results are discussed with respect to applied and fundamental research.
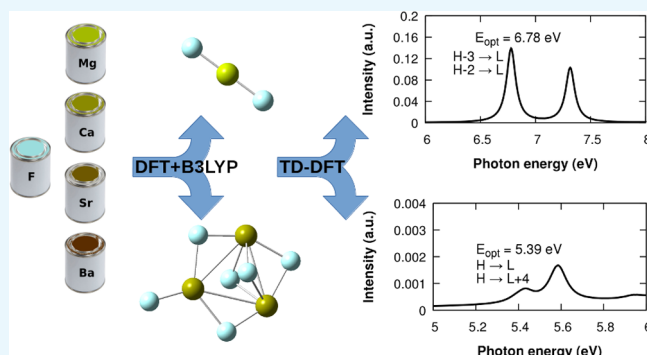
INTRODUCTION

For years, fluorides and fluorite-type crystals have attracted much interest for their intrinsic optical properties and their potential applications in optoelectronic devices, in particular for those operating in the ultraviolet (UV) region. CaF_2, e.g., has a direct band gap at the Γ point of 12.1 eV and an indirect gap estimated around 11.8 eV.[1] Calcium fluoride, as well as other difluorides, is a highly ionic system that adopts the cubic $Fm\bar{3}m$ crystal structure with three atoms per unit cell.[2]

Due to their importance for applied and basic research, experimental studies on CaF_2 and other difluorides have been carried out for decades. Different experimental techniques were applied to study the optical, structural, and electronic properties of these compounds, such as discharge tube experiments,[3] reflectance,[1] dielectric loss techniques,[4] photoelectron spectrometry measurements,[5] light absorption[6] and spectrophotometry techniques,[7] neutron diffraction,[8] and polarized-light methods.[9,10]

From the theoretical and computational point of view, the most recent results concern optical and electronic excitations. Linear and non-linear optical properties of insulators with a cubic structure (CaF_2, SrF_2, CdF_2, BaF_2) were calculated within the first-principles orthogonalized linear combination of atomic orbitals (OLCAO) method.[11] Other studies, focused on point defects in CdF_2, were performed within the plane wave-pseudopotential (PW-PP) method.[12] Electronic excitation and energy bands of CaF_2 and other fluorides were determined by the quasiparticle DFT-GW approach, using a plane wave basis set and ionic pseudopotentials, i.e., a PW-PP scheme.[13] Using the hybrid B3PW functional, the electronic structures of defected fluorides, namely, CaF_2 and BaF_2, were evaluated.[14−16] After an iterative procedure using an effective Hamiltonian, the imaginary part of the dielectric function ε_2 was calculated for CaF_2,[17] within a PW-PP scheme and considering a screened interaction for electron−hole (e−h) parts. Native and rare-earth-doped defect complexes in β-PbF_2 were studied by atomistic simulations.[18]

Bulk cubic fluorides have been investigated yet by some researchers of the present collaboration. Some of us investigated the cubic fluorides in detail by means of DFT within the local density approximation (LDA) for the exchange-correlation energy.[19] The ground-state electronic properties were calculated for the bulk cubic structures of CaF_2, SrF_2, BaF_2, CdF_2, HgF_2, and β-PbF_2, using a plane wave expansion of the wave functions. The results showed good agreement with existing experiments and previous theoretical predictions. General trends of the ground-state parameters, the
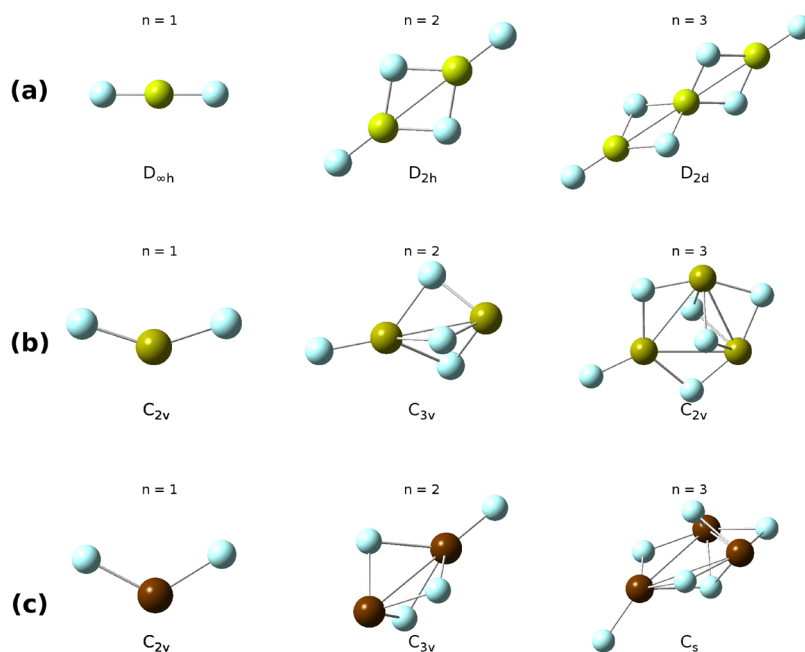
Figure 1. Structure of $(MF_2)_n$ clusters with n being the number of MF_2 units. The point group symmetry for each cluster is also reported. (a) M = Mg. (b) M = Ca, Sr. (c)M = Ba. Fluorine atoms are in cyan color, metal atoms in other colors.

electronic energy bands, and transition energies for all fluorides considered have been given and discussed in detail. Moreover, for the first time, results for HgF_2 were presented. In following works, the same authors studied the electronic and optical properties of two of the above bulk compounds, namely, CdF_2 and BaF_2, using state-of-the-art computational techniques for the one- and two-particle effects.[20,21] Also, in these cases, the obtained results were in good agreement with existing experimental data.

In the present paper, we face the problem of the calculation of the electronic and optical properties of the three smallest clusters of alkaline-earth metal fluorides, namely, MF_2 with M = Mg, Ca, Sr, Ba. The interest in these finite fluoride systems rises from the fact that clusters are the smallest pieces of matter that can exist in a stable form. Due to the small volume/surface ratio and the high number of unsaturated bonds, small clusters usually show different structural, electronic, and optical and reactive features with respect to their bulk parent compounds. They can be considered as prototypical examples of fragments of larger fluoride samples.

On the experimental side, it is known that in high-temperature vapors of alkaline-earth dihalides, monomers, dimers, and trimers (namely, MX_2, $(MX_2)_2$, $(MX_2)_3$ with M as the metal atom and X as the halide atom) are contained in.[22] While the monomers have already been studied either experimentally and theoretically, less information is available for dimers and trimers. For example, for the dimers, information has been obtained from infrared (IR) and Raman spectra of their vapors trapped in solid matrices.[23] For MgF_2 dimers and trimers, an extended comparison between Hartree−Fock/Moeller−Plesset calculations and experimental data has been performed by Francisco et al.[24] Studies on other families of fluoride clusters have been also performed: e.g., the lowest-energy isomers of coinage metal fluoride and chloride clusters have been analyzed systematically within a DFT scheme.[25]

The present study is further motivated by the recent interest on the electronic and optical properties of alkaline-earth metal fluoride clusters emerging in the literature.[26−29] Here, we focus on $(MX_2)_n$ systems with n = 1, 2, 3. Therefore, our attention is dedicated to subnanometric fluoride shards for the first smallest three members of each family for which larger deviations from the corresponding bulk solids in the structural, electronic, and optical properties are expected.

Therefore, the electronic and optical properties of the clusters will then be directly compared with their bulk counterparts.

RESULTS AND DISCUSSION

Ground State and Morphological Properties. In Figure 1, the geometrical structures of the clusters studied here are reported. According to the present calculations, only MgF_2 shows a linear structure with $D_{\infty h}$ point group symmetry. This finding is in accordance with the results of a recent paper by Pandey and coworkers.[28] On the other hand, for Ca, Sr, and Ba fluoride monomers, we find a bent configuration, with point symmetry group C_{2v}, in accordance with Levy and Hargittai,[26] Koput and Roszczak[27] (for CaF_2), and Calder et al.[29] In Table 1, our results for the M−F bond angles and distances of the monomers are in agreement with the results of Levy and Hargittai[26] with deviations within 2% (angles) and 0.5% (distances). The comparison of angles with experiments is also good.[29] On the contrary, Pandey and coworkers present linear geometries for all the monomers. A linear structure for Ca, Sr, and Ba fluoride monomers is neither confirmed here nor by other previous theoretical and experimental results.[26] Their conclusions on the structure of the monomers could be ascribed to the use of a less sophisticated basis set. This fact was addressed for CaF_2 by Koput and Roszczak[27] and for all the systems by Levy and Hargittai.[26]

Besides the case of the MgF_2 monomer, we also found differences with previous results in the case of $(BaF_2)_3$. In fact, $(BaF_2)_3$ clusters show a different geometry with respect to

Table 1. M−F^a Angles and Distances for the MF$_2$ Monomers after Present Calculations and after Other Calculations and Experiments^b

results	angle (°)	distance (Å)
CaF$_2$		
present	143.7	1.997
other-1	142.4	1.990
other-2	140	
SrF$_2$		
present	131.0	2.130
other-1	129.0	2.120
other-2	108	
BaF$_2$		
present	119.9	2.245
other-1	117.8	2.236
other-2	100	

^{a}M represents the metal atom and F the fluorine one. ^{b}Other-1 corresponds to results of calculations by Levy and coworkers with B3LYP XC functionals.[26] Other-2 corresponds to the M−F angles measured with the matrix isolation infrared spectroscopy technique (MI-IR).[29]

(CaF$_2$)$_3$ and (SrF$_2$)$_3$. According to our findings, the n = 3 Ba cluster belongs to the C_s point group symmetry, while this cluster is assigned to the C_{2v} group by Pandey and coworkers.[28]

It is well known from the literature[24,28] that (MF$_2$)$_n$, for n = 2, 3, shows many different local minima at energies as low as few tenths of eV over the ground state (global minimum), so we have performed a search for the lower-energy isomers, as outlined in the Supporting Information. The results show that the ground-state structures previously discussed are in fact the lowest-energy isomers.

It is interesting to analyze also the electronic properties of the ground state and their chemical trends. We refer to Table 2

Table 2. Ground-State Properties of the Fluoride Clusters^a

cluster	R_{M-F} [Å]	E_{frag} [eV]	IE$_V$ [eV]	EA$_V$ [eV]
MgF$_2$	1.747 (1.72)		12.94 (12.1)	0.45 (−0.4)
(MgF$_2$)$_2$	1.997 (2.06)	2.47 (3.6)	12.19 (11.5)	0.71 (−0.4)
(MgF$_2$)$_3$	1.867 (1.86)	2.56 (3.5)	11.91(11.3)	0.76 (−0.4)
CaF$_2$	1.997 (2.06)		11.52 (9.3)	0.69 (0.0)
(CaF$_2$)$_2$	2.166 (2.2)	2.67 (4.0)	11.08 (8.9)	1.03 (1.6)
(CaF$_2$)$_3$	2.187 (2.24)	2.83 (4.8)	10.68 (8.9)	0.84 (1.1)
SrF$_2$	2.130 (2.2)		10.94 (9.0)	0.78 (0.1)
(SrF$_2$)$_2$	2.316 (2.31)	2.56 (3.9)	10.55(10.2)	0.96 (1.4)
(SrF$_2$)$_3$	2.332 (2.38)	2.83 (4.7)	10.13 (8.8)	0.80 (0.3)
BaF$_2$	2.245 (2.33)		10.58 (8.1)	0.61 (3.6)
(BaF$_2$)$_2$	2.29 (2.47)	2.31(3.7)	9.93 (7.7)	0.69 (2.1)
(BaF$_2$)$_3$	2.56 (2.52)	2.58 (4.5)	9.70 (7.4)	0.56 (2.4)

^{a}The average distance between the metal and the fluorine atom R_{M-F}, the fragmentation energy E_{frag}, the vertical ionization energy IE$_V$, and vertical electron affinity EA$_V$ are listed. In parentheses, the corresponding data from the work of Pandey et al.[28] are given.

for these calculated observables. The average distance between the fluorine and metal atom within the clusters behaves differently in the case of the Mg fluoride clusters. In this case, the average distance is at a maximum for n = 2, while for all other clusters (Ca, Sr, and Ba), that observable is larger for n = 3. Our results compare well with those of Pandey and coworkers.[28] From these results, it seems that the larger is the

number of MF$_2$ units present in the cluster, the larger is the average distance between the metal and the fluorine atoms.

Another important observable for the molecules is their fragmentation energy, i.e., the energy required to remove an MF$_2$ unit from an (MF$_2$)$_n$ cluster[28]

$$E_{frag}(n) = E((MF_2)_{n-1}) + E(MF_2) - E((MF_2)_n) \quad (1)$$

where $E((MF_2)_n)$ represents the total ground-state energy of the cluster made by n MF$_2$ units. $E_{frag}(n)$ is the cost in energy to extract an MF$_2$ unit from an n-unit cluster. In contrast to the results of Pandey and coworkers, it seems that for n = 2, 3, the Mg fluoride clusters show a different behavior compared to the clusters with Ca, Sr, and Ba metal atoms. While in the latter cases, the fragmentation energy is larger at n = 3 by about 20%, in the case of the Mg fluoride clusters, this energy is almost the same for n = 2, 3.

The values for the fragmentation energies reported in Table 2 are of the same order of magnitude as those reported by the group of Pandey, even if slightly smaller. Passing from n = 2 to n = 3, for all the clusters considered here, one obtains larger energies for the creation of an MF$_2$ unit. For n = 2, the smallest fragmentation energy appears for the Ba fluoride cluster while the largest one occurs for the Ca clusters. For n = 3 the smallest fragmentation energy is reported for the Mg fluoride cluster, while the largest is found for the fluoride Ca and Sr clusters. The differences w.r.t. Pandey et al. could be a direct consequence of the different choices for the basis set, which led in some cases also to different ground-state geometries.[28]

The comparison of the vertical ionization energy and the vertical electron affinity is also interesting. These quantities are defined as

$$IE_V = E_C^0 - E_N^0 \quad (2)$$

$$EA_V = E_N^0 - E_A^0 \quad (3)$$

where E_N^0, E_A^0, and E_C^0 are defined above.

The MgF$_2$ clusters exhibit the largest IE$_V$, with calculated values around 12.3 eV, while for CaF$_2$, SrF$_2$, and BaF$_2$, the results and trends compare well with those reported by Pandey et al.[28] The ionization energy for the MgF$_2$ monomer, 12.94 eV, is also in fair agreement with experimental findings 13.3 ± 0.3 eV[24] and 13.6 ± 0.2 eV.[24] No clear trend is found for the absolute values of the vertical electron affinity EA$_V$, with values around 0.6 eV for MgF$_2$ and BaF$_2$ clusters and close to 0.8 eV for the remaining ones. This is in contrast to the values reported by Pandey and coworkers, who found a negative electron affinity for MgF$_2$ clusters. We remark that the evaluation of EA for clusters within DFT suffers per se of well-known problems. Even in the atomic case, electron affinities cannot be correctly obtained because the long-range behavior of the exchange-correlation potential is incorrect for negative ions.[30] These facts are related to the need to correctly consider self-interaction correction (SIC) terms of a system (molecule) to evaluate properly its corresponding EA.[31] Therefore, for this observable, the comparison with other results, obtained within different methods, could be less satisfactory.[32,33]

Electronic Excitations and Optical Properties. We turn here to the study of the electronic excitation properties, discussing the optical absorption spectra of the clusters. From total energy differences, it is possible to evaluate important electronic observables. In fact, the ΔSCF technique enables us

Table 3. Excited and Optical Properties of the Clusters[a]

cluster	E_{gap} [eV]	E_{opt} [eV]	E_b [eV]
MgF_2	12.49	**6.78** (0.14; H-3 → L, H-2 → L)	5.71
$(MgF_2)_2$	11.48	**6.56** (0.03; H-1 → L, H → L+1)	4.92
$(MgF_2)_3$	11.15	**6.66** (0.03; H-1 → L, H-1 → L+1, H → L)	4.49
CaF_2	10.90	**5.64** (5.9×10^{-5}; H → L)	5.19
$(CaF_2)_2$	10.04	**5.42** (1.9×10^{-4}; H-1 → L, H → L)	4.62
$(CaF_2)_3$	9.84	**5.39** (1.1×10^{-4}; H → L, H → L+4)	4.45
SrF_2	10.16	**5.26** (7.0×10^{-4}; H → L)	4.9
$(SrF_2)_2$	9.60	**5.11** (1.6×10^{-3}; H-2 → L)	4.49
$(SrF_2)_3$	9.33	**5.10** (4.0×10^{-4}; H-1 → L)	4.23
BaF_2	9.98	**5.40** (8.0×10^{-4}; H → L)	4.58
$(BaF_2)_2$	9.24	**5.25** (1.6×10^{-3}; H → L)	3.99
$(BaF_2)_3$	9.15	**5.40** (1.3×10^{-3}; H → L)	3.75

[a]The quasiparticle gap (E_{gap}), the optical onset (E_{opt} in bold), and the binding energy of the exciton (E_b) are given. In the third column, for E_{opt}, the oscillator strength of the transition followed by the states involved in the transition in the form initial state → final state with H for HOMO and L for LUMO states is given in parentheses.
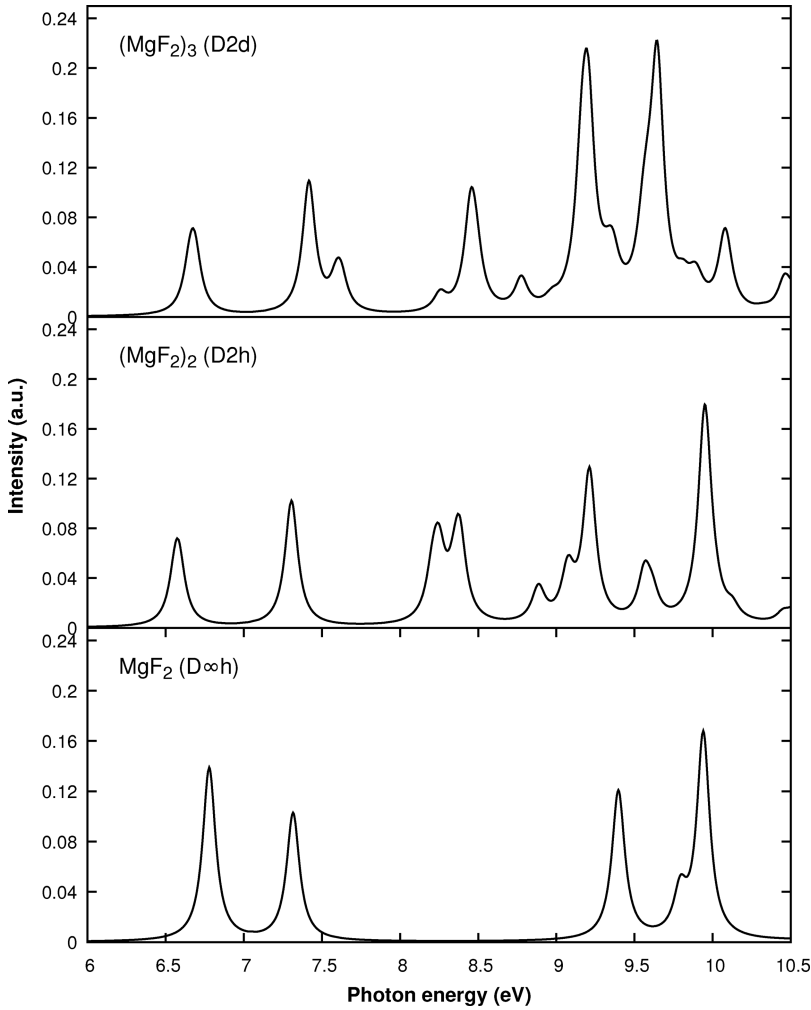

Figure 2. Optical absorption spectra for MgF_2 clusters.

to calculate the fundamental gap for each cluster. From the ΔSCF method, one obtains the quasiparticle gap (or fundamental gap) by the expression[34,35]

$$E_{gap} = IE_V - EA_V = (E_C^0 - E_N^0) - (E_N^0 - E_A^0) \quad (4)$$

Related to this, from the knowledge of the optical gap energy E_{opt}, defined as the first optically active transition in the absorption spectrum, an estimate of the exciton binding energy can be obtained through the difference $E_b = E_{gap} - E_{opt}$.

An exciton can be considered as an elementary excitation resulting from a bound state made of an electron and a hole. It is created as a consequence of the absorption of a photon; an electron and a hole are attracted to each other by the electrostatic Coulomb force. It can be considered as an
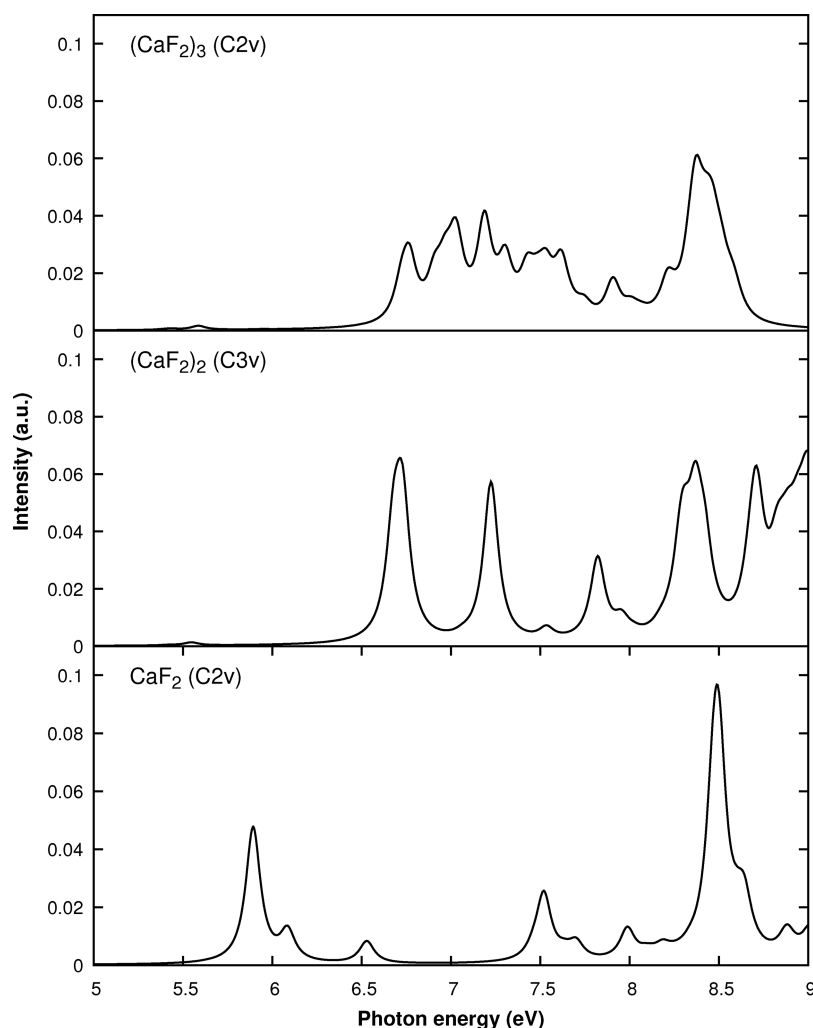
Figure 3. Optical absorption spectra for CaF_2 clusters.

electrically neutral quasiparticle that can exist in insulators and semiconductors that can transport energy without transporting net electric charge.[33,36]

The resulting QP energies from the equation of E_{gap} gap are reported in Table 3. The average values for each family are 10.7, 10.3, 9.7, and 9.4 eV, respectively, for MgF_2, CaF_2, SrF_2, and BaF_2 and exhibit a decreasing trend with increasing size of the metal atom; for a given metal atom, they decrease when going from $n = 1$ to $n = 3$ with a spread of about 1.0−0.75 eV.

Table 3 also reports additional information on the details and nature of the electronic transitions contributing to the onset. All clusters begin to absorb in the middle UV (MUV; 3.10−4.13 eV), and we study their spectra up to the far UV (FUV; 4.13−10.16 eV). Besides the Mg fluoride clusters, which show an average value of E_{opt} of about 6.7 eV, the other systems display average onset energies in the range of 5.1−5.5 eV. This observable shows very small variations with respect to n at a fixed cation. It is clear from Table 3 that while for the MgF_2 and CaF_2 clusters, the onset energies are determined by different transitions around the HOMO−LUMO gap, for the heaviest metal clusters (Sr and Ba), typically, only one transition enters in the first absorption peak. In particular, for all Ba clusters, the HOMO to LUMO transition is responsible for absorption at the optical onset.

Optical Absorption Spectra. The absorption spectra of all clusters were determined through the TDDFT scheme and are displayed in Figures 2−5. The details related to the onset energies are reported in Table 3.

Clear chemical and structural trends are visible. While the absorption onset increases going from Mg to Ba, the average absorption strength decreases. The number n of MX_2 units is related to the electronic confinement. In fact, the size of the cluster determines the importance of quantum confinement as it is clear from the trend of E_{gap} that is larger for smaller clusters. The absorption edge slightly shifts toward lower energies with increasing n. In the second column of the table, the oscillator strength of the transition followed by the states involved in the transition in the form initial state → final state with H for HOMO and L for LUMO states is reported in parentheses.

All the Mg systems present sharp peaks of absorption in the range 6.5−10.5 eV with intensites that are almost double w.r.t. the other MF_2 systems. Moreover, the absorption spectrum of the MgF_2 monomer displays a region 2 eV wide, from about 7.4 eV to about 9.4 eV in which the material is transparent. There is no analogous behavior in the other systems studied here.

Another important fact distinguishes the MgF_2 clusters: All the onsets have peak intensities comparable with the other
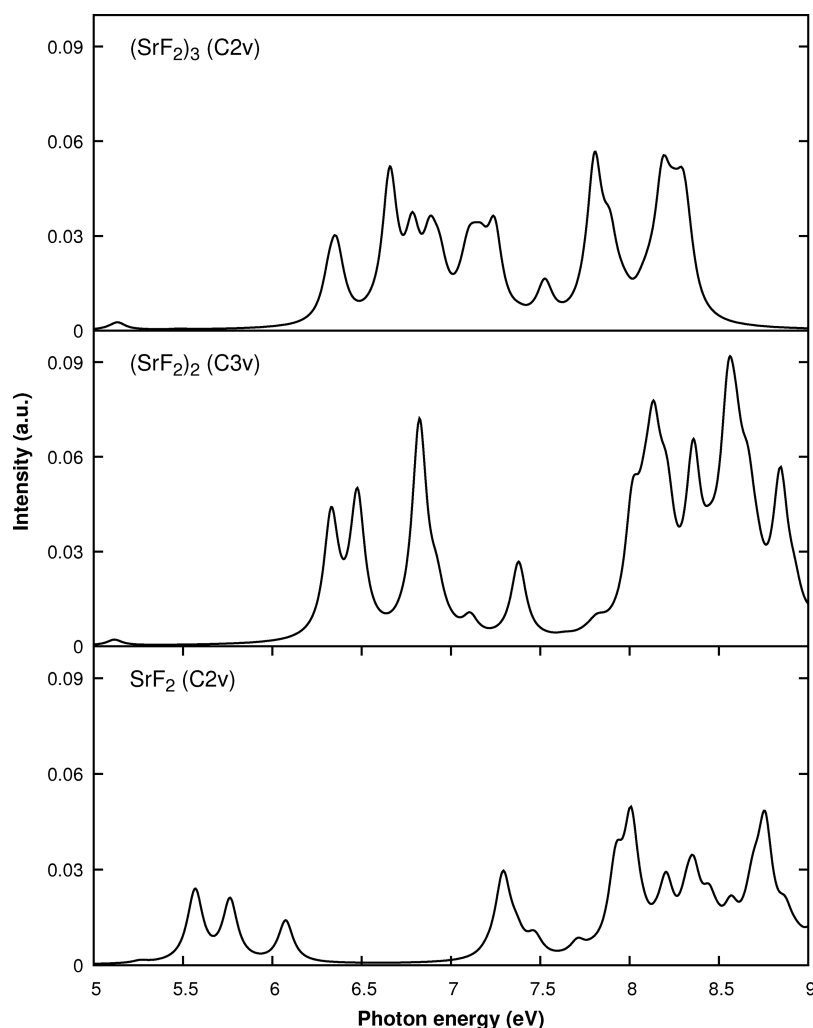
Figure 4. Optical absorption spectra for SrF_2 clusters.

structures of the spectrum. $(CaF_2)_n$, for $n = 2$, 3, and all SrF_2 and BaF_2 clusters only exhibit a tiny absorption structure at the onset in the range 5.1–5.6 eV, much weaker than the other absorption peaks at higher energy. In the case of CaF_2 monomer, the onset peak is located at a slightly higher energy in proximity of a stronger structure.

The differences in the absorption onsets and quasiparticle gaps are also listed in Table 3. They characterize the electron–hole binding in the lowest-energy exciton. The values for E_b are huge, of the order of 5 eV. They decrease slightly going from Mg to Ba. The decrease of E_b with n for a given cation illustrates the influence of electronic confinement on the electron–hole interaction.

Bulk Versus Cluster: Ground- and Excited-State Properties. The comparison between the ground- and excited-state properties of the clusters in Tables 2 and 3 and those of the corresponding bulk systems in Tables 4 and 5 may help to understand the effect of nanostructuring on electronic and optical properties. In Table 4, the ground- and excited-state properties of bulk cubic CaF_2 and BaF_2 are reported.[20,38] The computational schemes used to tackle bulk properties are DFT methods based on ionic pseudopotentials and a plane wave expansion of the electronic wave functions.[20,37] The reported observables are the distance between metal and fluorine atoms, R'_{M-F}, and the vertical ionization energy and

electron affinity, IE_V and EA_V, respectively. IE_V and EA_V are calculated as differences of energy levels for the (111) surface within a DFT-GGA scheme as difference of energy levels defining the vacuum level by the average electrostatic potential.[37] The quasiparticle gap (E_{gap}), the optical onset (E_{opt}), and the binding energy of the exciton (E_b) are reported as well. For these quantities, many-body techniques have been used. In Table 5, we summarize the excited and optical properties of bulk rutile (tetragonal) MgF_2.[39] It is clear from Table 4 that the average distance between the metal and the fluorine atom R_{M-F} in the clusters is larger than R'_{M-F} in the corresponding bulk systems. This can be ascribed to the fact that cluster systems are less constrained with respect to an infinite, translationally invariant bulk. IE_V and EA_V are smaller in Table 2 for the clusters than those in Table 4 for the bulk systems, implying that it is easier to extract electrons from or add electrons to molecules. As far as the excitation properties are concerned, the quasiparticle band gap energies of the clusters calculated here are smaller than in bulk but follow the same chemical trend. On the other hand, if we compare the energies of the optical onset, then we observe dramatic changes going from bulk to clusters. For example, the onset energy of MgF_2 (see Table 5) jumps from 10.9 eV (EUV) for bulk to an average value of 6.7 eV (FUV) for the clusters studied here. In the case of bulk CaF_2, the onset energy is 10.7 eV (EUV), and
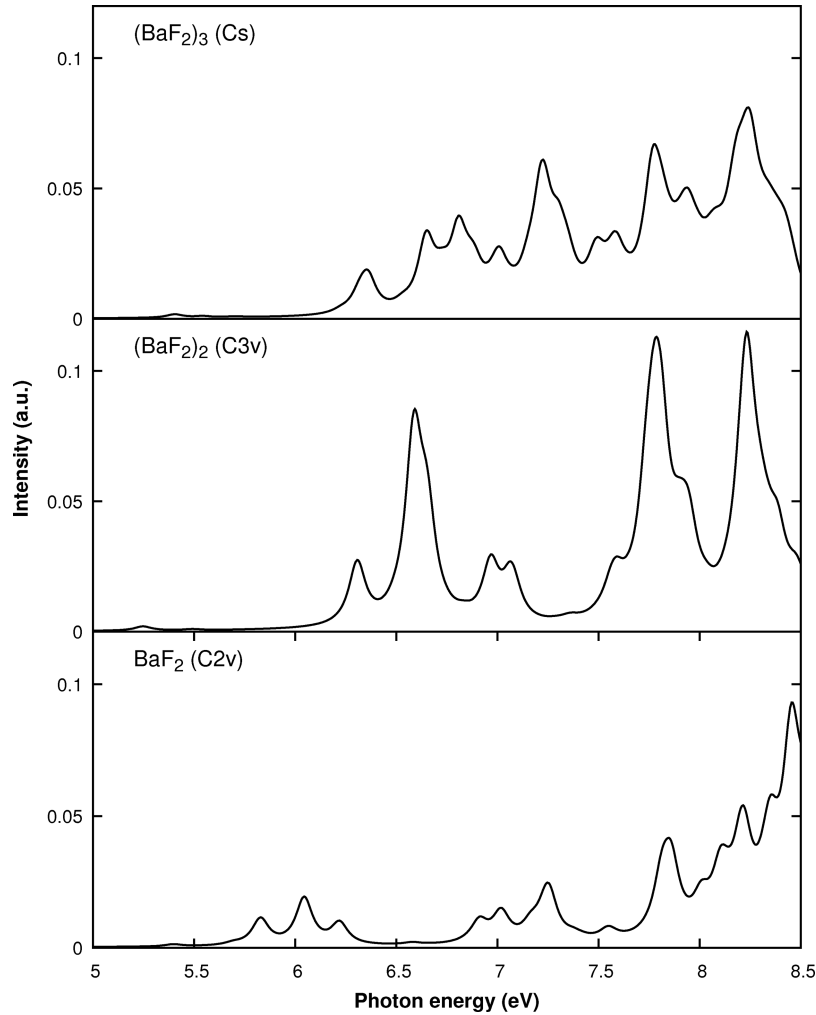
Figure 5. Optical absorption spectra for BaF$_2$ clusters.

Table 4. Ground-State, Excited-State, and Optical Properties for Bulk Cubic CaF$_2$ and BaF$_2$ Crystals[a]

solid	R'_{M-F}	IE$_V$ [eV]	EA$_V$ [eV]	E_{gap} [eV]	E_{opt} [eV]	E_b [eV]
CaF$_2$	2.35 (2.36)	11.84 (11.96)	1.04 (−0.15)	11.8 (12.1)	10.7 (11.2)	1.1 (0.9)
BaF$_2$	2.68 (2.68)	10.88 (10.7)	0.87 (0.21)	11.58 (11.0)	10.0 (10.0)	1.5 (1.0)

[a]In the left part of the panel—the distance between metal and fluorine atoms, R'_{M-F}, and the vertical ionization energy and electron affinity, IE$_V$ and EA$_V$, respectively. In parentheses, the experimental values for each observable are listed. IE$_V$ and EA$_V$ are calculated for the (111) surface. These data are taken from a work of Matusalem and coworkers.[37] The quasiparticle energy gap (E_{gap}), the optical onset (E_{opt}), and the binding energy of the exciton (E_b) are reported in the right side of the panel. In parentheses, the experimental values for each observable are reported. These quantities are referred to the fundamental direct transition for each bulk material. The data for CaF$_2$ are from a paper of Ma and Rohlfing[38] while those for BaF$_2$ are from a more recent work.[20]

Table 5. Excited and Optical Properties for Bulk MgF$_2$ Crystals[a]

solid	E_{gap} [eV]	E_{opt} [eV]	E_v [eV]
MgF$_2$	12.17 (12.4)	10.90 (11.2)	1.127 (1.2)

[a]This crystal has the rutile structure. These data are taken a work of Yi and Jia.[39] The quasiparticle gap (E_{gap}), the optical onset (E_{opt}), and the binding energy of the exciton (E_b) are reported. In parentheses, the experimental values for each observable as quoted in the same reference are reported. These quantities are referred to the fundamental direct transition of MgF$_2$.

the average value for the corresponding clusters is 5.4 eV (MUV). Therefore, the onset energies in the case of the clusters belong to a different UV domain with respect to their corresponding bulk systems. This fact can be ascribed to the presence of molecular transitions in clusters at energies for which the bulk system does not allow electronic transitions.

The large differences in E_{gap} and E_{opt} between clusters and bulk have an important consequence on the exciton binding energy, which results in strongly amplified in clusters. This fact can be ascribed to the interplay between confinement effects and reduced screening taking place in the finite systems. The results therefore suggest that there is a clear optical signature of the formation of clusters or other nanostructures or fragments compared to the bulk in the case of fluorides: the strongly reduced optical onset energy and the high exciton binding energy. The presence of these effects produces an optical signature of the formation of such molecular systems, e.g., in an

347 optical absorption experiment for fluorides. Therefore, these
348 two facts may have application-related consequences. The
349 important message for possible UV applications is that the
350 optical absorption of the fluoride clusters starts in an energy
351 region, the MUV one, which is much below the optical onset
352 regions of their corresponding solids, which absorb the FUV
353 part of the spectrum. This means that the same material, a
354 fluoride compound, if prepared as a (small) cluster or as a bulk
355 crystal, shows very different UV properties with possibly very
356 different application-related consequences for UV devices.

357 Here, we studied only small clusters and showed that their
358 electronic and optical properties are very different in
359 comparison to bulk crystals. It could be interesting to find
360 out if the same scenario shows up for larger fluoride molecules,
361 which are expected to resemble more the electronic and optical
362 behavior of the solid phase. We postpone this point to a
363 forthcoming study on these systems.

364 ## ■ CONCLUSIONS

365 We presented a systematic investigation on the electronic and
366 optical properties of the first three smallest stable clusters of
367 fluoride compounds, namely, MgF_2, CaF_2, SrF_2, and BaF_2. We
368 compared several electronic and optical properties for clusters
369 of different sizes with the same metal atom and for clusters of
370 the same size with different metal atoms. From this analysis, it
371 turns out that MgF_2 clusters are predicted to have
372 distinguished ground- and excited-state properties with respect
373 to the other fluoride systems studied here. Moreover,
374 comparing the optical properties of the three cluster classes
375 with those of the corresponding bulk fluorides, two important
376 features are clearly visible: In the case of the clusters, a strong
377 redshift of the onset energy and a corresponding rise of the
378 exciton binding energy with respect to the bulk cases are
379 observed. These effects, aside from their importance in the
380 ongoing basic research on fluorides, turn out to be important
381 for possible applications. Their presence/absence could be
382 used as a discriminating/sorting criterion in optical measure-
383 ments to check the formation and presence of such fragments
384 in the target.

385 ## ■ COMPUTATIONAL METHODS

386 For the case of $(MX_2)_n$ clusters treated here, with respect to
387 geometry optimization, one has to consider an appropriate
388 basis set due to the presence of fluorine and metal atoms of the
389 second group. For all the clusters studied, different choices of
390 the basis sets are reported in the literature.[26−29] Here, we
391 employ def2-QZVPPD[40] for all atoms, i.e., the Karlsruhe
392 quadruple-ζ valence basis set with polarization functions[41] and
393 the addition of moderately diffuse basis functions.[42] The
394 capability of this basis set to reproduce several properties (e.g.,
395 dipole polarizabilities, transition dipole moments, Raman
396 intensities, optical rotations, and non-linear optical coeffi-
397 cients) of different clusters with high accuracy has been widely
398 demonstrated.[41,42]

399 For Sr and Ba atoms, inner-shell electrons are modeled by
400 effective core potentials (ECP), which reduce the required
401 basis set size and account for relativistic effects.[41] ECPs deliver
402 the accuracy of all-electron calculations with considerable
403 reduction of the computational load, as shown in a work of
404 Kaupp and coworkers.[43]

405 Our approach substantially differs from the recent study of
406 Pandey and coworkers where the LanL2DZ and 6-31G* basis

407 sets were used for alkaline-earth metal and fluorine atoms,
408 respectively.[28]

409 With respect to the exchange-correlation (XC) potential, we
410 chose the B3LYP one since with respect to other possibilities,
411 e.g., the Perdew−Burke−Ernzerhof (PBE) functional, it
412 reproduces better results for different clusters, e.g., for many
413 PAH molecules, for both ground and excited states, as
414 previously established.[33−36]

415 We perform all the DFT and time-dependent DFT
416 (TDDFT) calculations using the Gaussian16 computational
417 code, an all-electron Gaussian-based package.[44] This code
418 enables us to characterize different clusters with respect to
419 ground-state and excited-state properties.[34,35] In particular, the
420 ground-state and the electronic properties, e.g., fragmentation
421 energies, electron affinities, ionization energies, and quasipar-
422 ticle (QP) gaps, are obtained here through the DFT method
423 for all the fluoride molecules analyzed. Second, the time-
424 dependent counterpart of this scheme allows the calculation of
425 the optical properties (optical onsets, exciton binding energies)
426 and to work out the absorption spectra from the visible up to
427 the UV range covering the middle ultraviolet (MUV [4.13−
428 6.20 eV]) and part of the far ultraviolet (FUV [6.20−10.16
429 eV]) spectral range. In particular, the Casida computational
430 scheme is used for the calculations of the poles of the
431 polarizability function in the frequency domain. These poles
432 correspond to vertical excitation energies, whereas their
433 strengths represent the oscillator strengths of the involved
434 transitions.[45,46] Finally, we use the ΔSCF scheme[47,48] to
435 calculate the vertical electron affinities (EA_V) and ionization
436 energies (IE_V) as differences between the ground-state total
437 energy of the neutral system, E_N^0, and the energies of the
438 charged clusters (the anion E_A^0 and the cation E_C^0), keeping
439 fixed at the neutral geometry.

440 All the spectra presented here are calculated within TDDFT,
441 including exchange and correlation effects in the B3LYP
442 approximation.[45,49] The comparison of TDDFT calculations
443 with experimental data is typically very good for small
444 clusters.[32,50,51] In particular, in the present work, we are
445 mainly interested in studying trends in the optical absorption
446 of families of fluoride clusters. Therefore, the TDDFT scheme
447 turns out to be particularly advisable, efficient, and
448 reliable.[33,36,52]

■ ASSOCIATED CONTENT

449

⒮ **Supporting Information** 450

The Supporting Information is available free of charge at 451
https://pubs.acs.org/doi/10.1021/acsomega.0c01317. 452

> Configurational effects on the spectra and energy 453
> stability of the ground state (PDF) 454

■ AUTHOR INFORMATION

455

Corresponding Author 456

> **Giancarlo Cappellini** − *Department of Physics, University of* 457
> *Cagliari, Cittadella Universitaria di Monserrato, 09042* 458
> *Monserrato, Italy;* ⊙ orcid.org/0000-0001-9746-3025; 459
> Email: giancarlo.cappellini@dsf.unica.it 460

Authors 461

> **Andrea Bosin** − *Department of Physics, University of Cagliari,* 462
> *Cittadella Universitaria di Monserrato, 09042 Monserrato,* 463
> *Italy* 464

Giovanni Serra − *Department of Physics, University of Cagliari, Cittadella Universitaria di Monserrato, 09042 Monserrato, Italy*

Jürgen Furthmüller − *ETSF and IFTO, FSU-Jena, D-07743 Jena, Germany*

Friedhelm Bechstedt − *ETSF and IFTO, FSU-Jena, D-07743 Jena, Germany*

Silvana Botti − *ETSF and IFTO, FSU-Jena, D-07743 Jena, Germany;* orcid.org/0000-0002-4920-2370

Complete contact information is available at:
https://pubs.acs.org/10.1021/acsomega.0c01317

Notes

The authors declare no competing financial interest.

■ REFERENCES

(1) Rubloff, G. W. Far-Ultraviolet Reflectance Spectra and the Electronic Structure of Ionic Crystals. *Phys. Rev. B* **1972**, *5*, 662−684.

(2) Zemann, J. Crystal structures,2nd edition. Vol. 1by R. W. G. Wyckoff. *Acta Crystallogr.* **1965**, *18*, 139−139.

(3) Tousey, R. Optical Constants of Fluorite in the Extreme Ultraviolet. *Phys. Rev.* **1936**, *50*, 1057−1066.

(4) Samara, G. A. Temperature and pressure dependences of the dielectric properties of PbF_2 and the alkaline-earth fluorides. *Phys. Rev. B* **1976**, *13*, 4529−4544.

(5) Scrocco, M. Satellites in x-ray photoelectron spectroscopy of insulators. I. Multielectron excitations in CaF_2, SrF_2, and BaF_2. *Phys. Rev. B* **1985**, *32*, 1301−1305.

(6) Weesner, F. J.; Wright, J. C.; Fontanella, J. J. Laser spectroscopy of ion-size effects on point-defect equilibria inPbF_2:Eu^{3+}. *Phys. Rev. B* **1986**, *33*, 1372−1380.

(7) Kosacki, I.; Langer, J. M. Fundamental absorption edge of PbF_2 and $Cd_{1-x}Pb_xF_2$ crystals. *Phys. Rev. B* **1986**, *33*, 5972−5973.

(8) Hull, S.; Keen, D. A. Effect of hydrostatic pressure on the crystal structure and superionic behavior of lead (II) fluoride. *Phys. Rev. B* **1998**, *58*, 14837−14844.

(9) Fujita, M.; Itoh, M.; Bokumoto, Y.; Nakagawa, H.; Alov, D. L.; Kitaura, M. Optical spectra and electronic structures of lead halides. *Phys. Rev. B* **2000**, *61*, 15731−15737.

(10) Burnett, J. H.; Levine, Z. H.; Shirley, E. L. Intrinsic birefringence in calcium fluoride and barium fluoride. *Phys. Rev. B* **2001**, *64*, 241102R.

(11) Ching, W. Y.; Gan, F.; Huang, M.-Z. Band theory of linear and nonlinear susceptibilities of some binary ionic insulators. *Phys. Rev. B* **1995**, *52*, 1596−1611.

(12) Mattila, T.; Pöykkö, S.; Nieminen, R. M. Ab initio study of point defects in CdF_2. *Phys. Rev. B* **1997**, *56*, 15665−15671.

(13) Shirley, E. L. Many-body effects on bandwidths in ionic, noble gas, and molecular solids. *Phys. Rev. B* **1998**, *58*, 9579−9583.

(14) Jia, R.; Shi, H.; Borstel, G. The atomic and electronic structure of CaF_2 and BaF_2 crystals with H centers: a hybrid DFT calculation study. *J. Phys.: Condens. Matter* **2010**, *22*, No. 055501.

(15) Shi, H.; Eglitis, R. I.; Borstel, G. Ab initio calculations of the BaF_2 bulk and surface F centers. *J. Phys.: Condens. Matter* **2006**, *18*, 8367−8381.

(16) Shi, H.; Eglitis, R. I.; Borstel, G. Ab initio calculations of the CaF_2 electronic structure and F centers. *Phys. Rev. B* **2005**, *72*, No. 045109.

(17) Benedict, L. X.; Shirley, E. L. Ab initio calculation of $\epsilon_2(\omega)$ including the electron-hole interaction: Application to GaN and CaF_2. *Phys. Rev. B* **1999**, *59*, 5441−5451.

(18) Jiang, H.; Costales, A.; Blanco, M. A.; Gu, M.; Pandey, R.; Gale, J. D. Theoretical study of native and rare-earth defect complexes in β-PbF_2. *Phys. Rev. B* **2000**, *62*, 803−809.

(19) Cadelano, E.; Cappellini, G. Electronic structure of fluorides: general trends for ground and excited state properties. *Eur. Phys. J. B* **2011**, *81*, 115−120.

(20) Cadelano, E.; Furthmüller, J.; Cappellini, G.; Bechstedt, F. One- and two-particle effects in the electronic and optical spectra of barium fluoride. *J. Phys.: Condens. Matter* **2014**, *26*, 125501.

(21) Cappellini, G.; Furthmüller, J.; Cadelano, E.; Bechstedt, F. Electronic and optical properties of cadmium fluoride: The role of many-body effects. *Phys. Rev. B* **2013**, *87*, No. 075203.

(22) Berkowitz, J.; Marquart, J. R. Mass-Spectrometric Study of the Magnesium Halides. *J. Chem. Phys.* **1962**, *37*, 1853−1865.

(23) Lesiecki, M. L.; Nibler, J. W. Infrared and Raman spectra and structures of matrix isolated magnesium dihalides: MgF_2, $MgCl_2$, $MgBr_2$, and MgI_2. *J. Chem. Phys.* **1976**, *64*, 871−884.

(24) Francisco, E.; Costales, A.; Martin Pendás, A. Structure and Bonding in Magnesium Difluoride Clusters: The MgF_2 Molecule. *J. Phys. Chem. A* **2001**, *105*, 4126−4135.

(25) Rabilloud, F. Structure and stability of coinage metal fluoride and chloride clusters (M_nF_n and M_nCl_n, M = Cu, Ag, or Au n = 1-6). *J. Comput. Chem.* **2012**, *33*, 2083−2091.

(26) Levy, J. B.; Hargittai, M. Unusual Dimer Structures of the Heavier Alkaline Earth Dihalides: A Density Functional Study. *J. Phys. Chem. A* **2000**, *104*, 1950−1958.

(27) Koput, J.; Roszczak, A. CaF_2 As a Quasilinear Molecule: the Vibrational-Rotational Energy Levels Predicted by Ab Initio Quantum Chemistry Approach. *J. Phys. Chem. A* **2004**, *108*, 9267−9273.

(28) Pandey, R. K.; Waters, K.; Nigam, S.; He, H.; Pingale, S. S.; Pandey, A. C.; Pandey, R. A theoretical study of structural and electronic properties of alkaline-earth fluoride clusters. *Comput. Theor. Chem.* **2014**, *1043*, 24−30.

(29) Calder, V.; Mann, D. E.; Seshadri, K. S.; Allavena, M.; White, D. Geometry and Vibrational Spectra of Alkaline-Earth Dihalides. II. CaF_2, SrF_2, and BaF_2. *J. Chem. Phys.* **1969**, *51*, 2093−2099.

(30) Filippetti, A. Electron affinity in density-functional theory in the local-spin-density approximation. *Phys. Rev. A* **1998**, *57*, 914−919.

(31) Toher, C.; Sanvito, S. Efficient Atomic Self-Interaction Correction Scheme for Nonequilibrium Quantum Transport. *Phys. Rev. Lett.* **2007**, *99*, No. 056801.

(32) Malloci, G.; Cappellini, G.; Mulas, G.; Mattoni, A. A (time-dependent) density functional theory study of the optoelectronic properties of bis-triisopropylsilylethynyl functionalized acenes. *Thin Solid Films* **2013**, *543*, 32−34.

(33) Cardia, R.; Malloci, G.; Rignanese, G.-M.; Blase, X.; Molteni, E.; Cappellini, G. Electronic and optical properties of hexathiapentacene in the gas and crystal phases. *Phys. Rev. B* **2016**, *93*, 235132.

(34) Mocci, P.; Cardia, R.; Cappellini, G. Si-atoms substitutions effects on the electronic and optical properties of coronene and ovalene. *New J. Phys.* **2018**, *20*, 113008.

(35) Mocci, P.; Cardia, R.; Cappellini, G. A computational study on the electronic and optical properties of boron-nitride circumacenes. *Phys. Chem. Chem. Phys.* **2019**, *21*, 16302−16309.

(36) Dardenne, N.; Cardia, R.; Li, J.; Malloci, G.; Cappellini, G.; Blase, X.; Charlier, J.-C.; Rignanese, G.-M. Tuning Optical Properties of Dibenzochrysenes by Functionalization: A Many-Body Perturbation Theory Study. *J. Phys. Chem. C* **2017**, *121*, 24480−24488.

(37) Matusalem, F.; Marques, M.; Teles, L. K.; Filippetti, A.; Cappellini, G. Electronic properties of fluorides by efficient approximated quasiparticle DFT-1/2 and PSIC methods: BaF_2, CaF_2 and CdF_2 as test cases. *J. Phys.: Condens. Matter* **2018**, *30*, 365501.

596 (38) Ma, Y.; Rohlfing, M. Quasiparticle band structure and optical
597 spectrum of CaF2. *Phys. Rev. B* **2007**, *75*, 205114.

598 (39) Yi, Z.; Jia, R. Quasiparticle band structures and optical
599 properties of magnesium fluoride. *J. Phys.: Condens. Matter* **2012**, *24*,
600 No. 085602.

601 (40) Pritchard, B. P.; Altarawy, D.; Didier, B.; Gibson, T. D.;
602 Windus, T. L. New Basis Set Exchange: An Open, Up-to-date
603 Resource for the Molecular Sciences Community. *J. Chem. Inf. Model.*
604 **2019**, *59*, 4814−4820.

605 (41) Weigend, F.; Ahlrichs, R. Balanced basis sets of split valence,
606 triple zeta valence and quadruple zeta valence quality for H to Rn:
607 Design and assessment of accuracy. *Phys. Chem. Chem. Phys.* **2005**, *7*,
608 3297.

609 (42) Rappoport, D.; Furche, F. Property-optimized Gaussian basis
610 sets for molecular response calculations. *J. Chem. Phys.* **2010**, *133*,
611 134105.

612 (43) Kaupp, M.; Schleyer, P. v. R.; Stoll, H.; Preuss, H.
613 Pseudopotential approaches to Ca, Sr, and Ba hydrides. Why are
614 some alkaline earth MX_2 compounds bent? *J. Chem. Phys.* **1991**, *94*,
615 1360−1366.

616 (44) Frisch, M. J.; et al. *Gaussian 16*; Revision C.01., Gaussian Inc.:
617 Wallingford CT, 2016.

618 (45) Casida, M. E. Time-Dependent Density Functional Response
619 Theory for Molecules. *Recent adv. Density Funct. Methods* **1995**, 155−
620 192.

621 (46) Jamorski, C.; Casida, M. E.; Salahub, D. R. Dynamic
622 polarizabilities and excitation spectra from a molecular implementa-
623 tion of time-dependent density-functional response theory: N_2 as a
624 case study. *J. Chem. Phys.* **1996**, *104*, 5134−5147.

625 (47) Malloci, G.; Cappellini, G.; Mulas, G.; Satta, G. Quasiparticle
626 effects and optical absorption in small fullerenelike GaP clusters. *Phys.*
627 *Rev. B* **2004**, *70*, 205429.

628 (48) Jones, R. O.; Gunnarsson, O. The density functional formalism,
629 its applications and prospects. *Rev. Mod. Phys.* **1989**, *61*, 689−746.

630 (49) Chong, D. P. *Recent Advances in Density Functional Methods*;
631 WORLD SCIENTIFIC: 1995.

632 (50) Sancho-García, J. C. Assessment of density-functional models
633 for organic molecular semi-conductors: The role of Hartree−Fock
634 exchange in charge-transfer processes. *Chem. Phys.* **2007**, *331*, 321−
635 331.

636 (51) Malloci, G.; Cappellini, G.; Mulas, G.; Mattoni, A. Electronic
637 and optical properties of families of polycyclic aromatic hydrocarbons:
638 A systematic (time-dependent) density functional theory study. *Chem.*
639 *Phys.* **2011**, *384*, 19−27.

640 (52) Körbel, S.; Boulanger, P.; Duchemin, I.; Blase, X.; Marques, M.
641 A. L.; Botti, S. Benchmark Many-Body GW and Bethe−Salpeter
642 Calculations for Small Transition Metal Molecules. *J. Chem. Theory*
643 *Comput.* **2014**, *10*, 3934−3943.